Supporting Information

Approaching Optimal Hole Transport Layers by Organic Monomolecular Strategy for Efficient Inverted Perovskite Solar Cells

Wang Li,[1,2]† Hui Liu,[1,2]† Changwen Liu,[1,2]† Weiguang Kong,[1,2] Hong Chen,[1,2] Weijun Wang,[1,2] Haichao Zhang,[1,2] Xian Zhang,[1,2] Chun Cheng[1,2]*

[1]Department of Materials Science and Engineering, Southern University of Science and Technology (SUSTech), Shenzhen, 518055, China
[2]Shenzhen Engineering Research and Development Center for Flexible Solar Cells, Southern University of Science and Technology (SUSTech), Shenzhen, 518055, China
E-mail: chengc@sustech.edu.cn
†These authors contributed equally.

Experimental Section

Materials and Methods: Indium tin oxide (ITO, 15 Ω sq^{-1}) glasses were purchased from Ying Kou You Xuan Trade Co. Ltd., China. PbI_2 (99.9985%) was purchased from Alfa Aesar, United States. PEDOT:PSS (Baytron PVP Al 4083) was bought from Baytron Company. TAPC, PTAA, MAI, $PbCl_2$, C_{60} and BCP were purchased from Xi'an Polymer Light Technology Corp, China. All solvents, such as N, N-dimethylformamide (DMF), isopropanol (IPA), chlorobenzene (CB), and dimethyl sulfoxide (DMSO) were purchased from Sigma-Aldrich, United States. These materials were used without purification.

Device fabrication: ITO glasses were cleaned in detergent, deionized water, IPA and ethanol for 15 min each by consecutive sonication. After drying with nitrogen flow, ITO glasses were treated by UV-ozone treatment for 10 min. PEDOT:PSS (filtered by a 0.45 μm filter) was spin coated onto the precleaned ITO substrates at 6000 rpm for 45s. After that, substrates were moved into glovebox. TAPC (10 mg/ml dissolved in CB) and PTAA (2 mg/ml dissolved in CB) were spin coated onto the pre-cleaned ITO substrates at 4000 rpm for 25s. All the p-HTLs were annealed at 110 ℃ for 10 min. For the preparation of ML-HTLs, CB was used to wash the p-TAPC and p-PTAA films, while deionized water was used to rinse away the redundant PEDOT:PSS. The prepared ML-HTLs were used directly for perovskite deposition. The perovskite precursor solution was prepared by dissolving 497.88 mg PbI_2, 33.37 mg $PbCl_2$, and 190.8 mg MAI in 0.9 mL DMF and 0.1 mL DMSO mixed solvent. The precursor was dripped on the ITO substrates and spin-coated at 700 rpm for 2s and 4000 rpm for 25s. 100 μL of CB was dripped within 1s onto the substrate at 18s before the

end. Then, the film was annealed at 105 ℃ for 5 min. Finally, C_{60} (40 nm), BCP (8 nm), and Ag (100 nm) were sequentially deposited on the perovskite film by thermal evaporation through a shadow mask with a defined active area of 0.10 cm^2.

Characterizations: All measurements were done at room temperature (298 K) and all samples in each test were measured in the same conditions. The thickness of films was measured by Dektak 8 Stylus Profiler. The morphology of perovskite and HTL films were characterized by scanning electron microscopy (SEM, TESCAN MIRA3), the electron beam is accelerated at 5 kV. Atomic force microscope (AFM) images of HTLs films were collected on a multimode SPM (Bruker) with tapping mode. The thickness was further measured using a dual rotating-compensator (Horibar-UVISEL ellipsometer, SUSTech CRF, Shenzhen, China). UPS analysis was conducted on the X-ray photoelectron spectrometer (Thermo Fischer, ESCALAB 250Xi) with an unfiltered He I (21.22 eV) gas discharge lamp and a hemispherical analyzer. Steady-state and time-resolved PL spectra were measured using an Edinburgh FLS5 spectroscopy system, and the pulsed laser wavelength was 405 nm. The excitation density of 5 nJ/cm^2 was used to avoid nonlinear effects. Photocurrent density-voltage (*J-V*) curves were measured under AM 1.5 G one sun illumination (100 mW/cm^2) with a solar simulator (Enlitech SS-F7-3A) equipped with a 300 W Xenon lamp and a Keithley 2400 source meter. For scan test, the J-V curves were tested from 1.2 to 0 V and 0 to 1.2 V with a scan velocity of 100 mV s^{-1}. For steady-state test, the voltage is fixed on the maximum power point to test the current output for all the test time. The light intensity was calibrated by NREL-calibrated Si solar cell. During measurement, the cell was covered by a mask with 0.1 cm^2 aperture. The external quantum efficiency (EQE) values were measured using an EQE system (Enlitech QE-R3011) containing a Xenon lamp, a monochromator, a Si detector for calibration, and a dual-channel power.
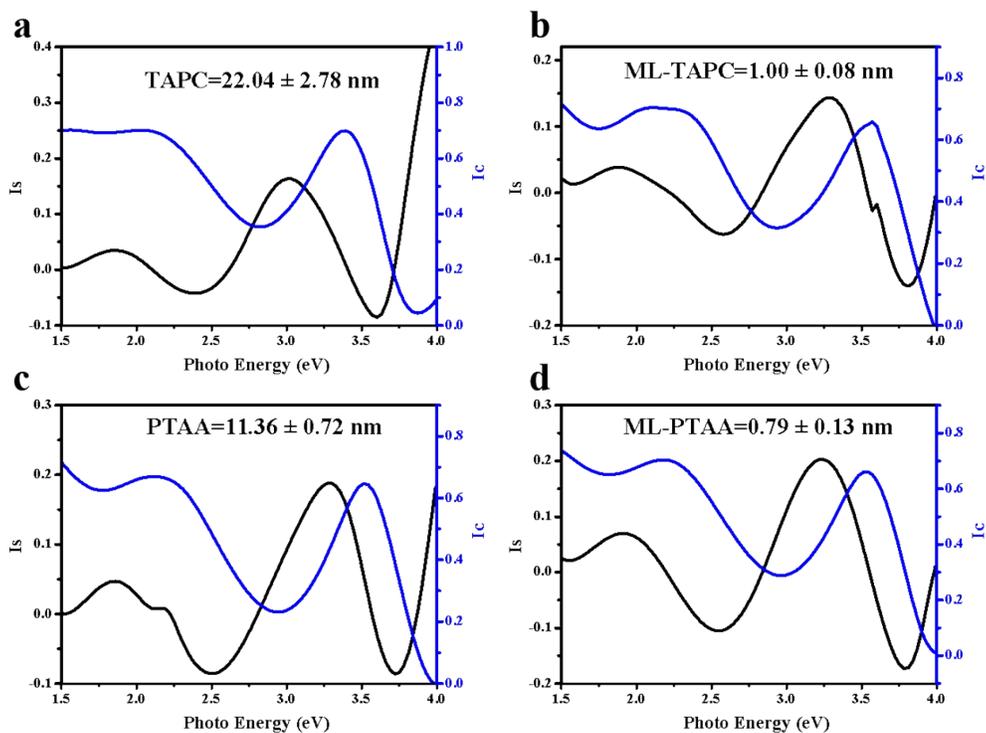
Figure S1. The thicknesses of (a) TAPC, (b) ML-TAPC, (c) PTAA and (d) ML-PTAA layer measured by ellipsometer.
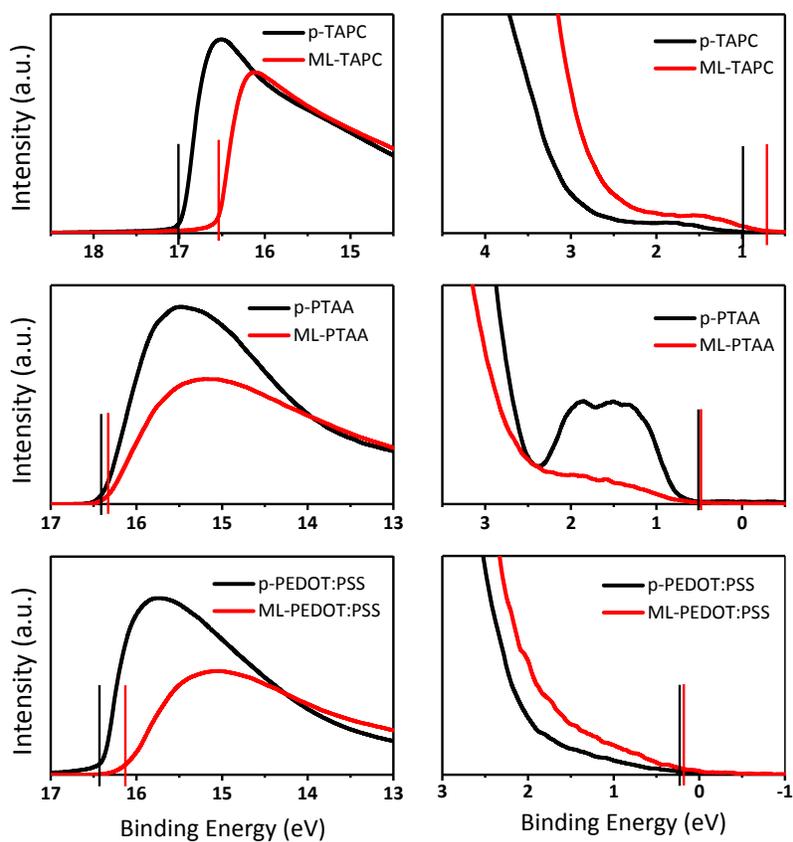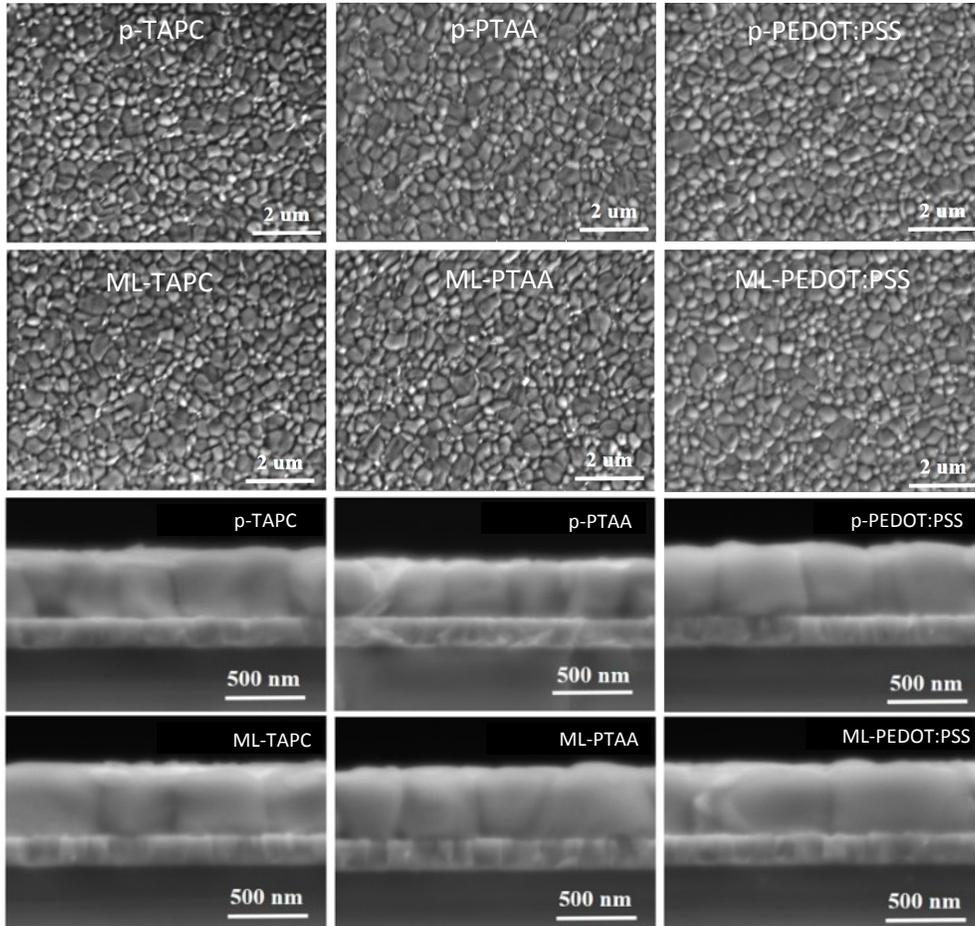
Figure S3. Top (4000×) and cross-sectional (20000×) view of SEM images of perovskite films on p-HTLs and ML-HTLs.

The SEM images reveal that the as-formed $MAPbI_{3-x}Cl_x$ films on HTLs exhibit similar morphologies, for example, uniform, compact and with similar grain size.
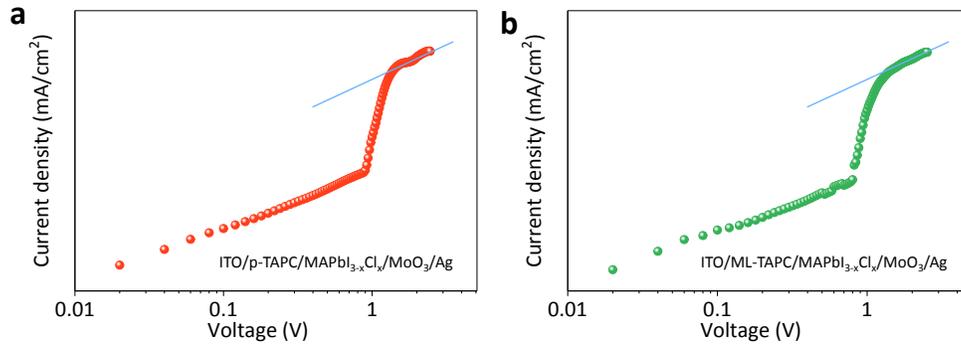
Figure S4. SCLC analysis of hole-only devices based on (a) p-TAPC and (b) ML-TAPC.

The hole mobility can be calculated in the SCLC region according to Mott-Gurney law,

$$J = \frac{9}{8}\varepsilon_0\varepsilon_r\mu\frac{V^2}{L^3}$$

where ε_r = 25 and L = 300 nm. For hole-only devices based on p-TAPC and ML-TAPC, the calculated mobility (μ) is both 3.7 × 10^{-2} $cm^2V^{-1}s^{-1}$.
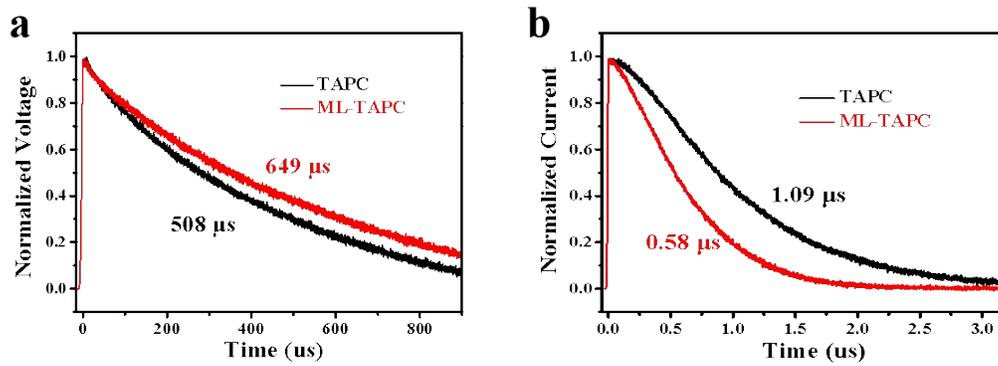
Figure S5. (a) Transient photovoltage and (b) transient photocurrent measurements for TAPC- and ML-TAPC-based PSCs.

5
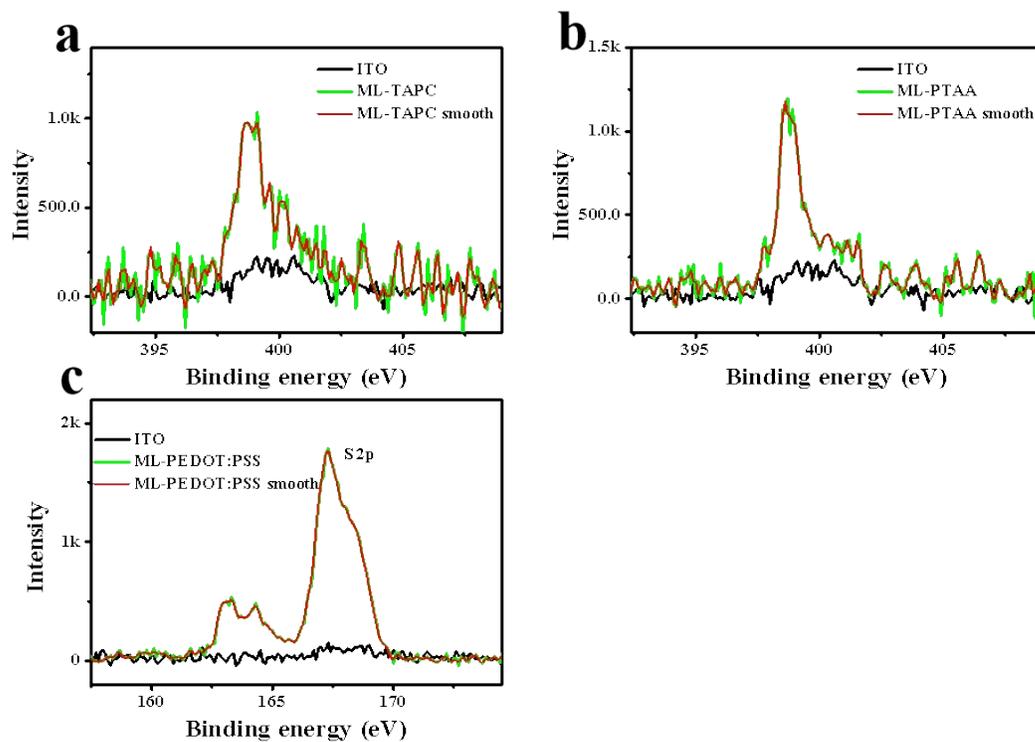
Figure S6. XPS spectra of (a) N 1s of ML-TAPC, (b) N 1s of ML-PTAA, and (c) S 2p of ML-PEDOT:PSS.

Table S1. E_f and HOMO values of p-HTLs and ML-HTLs obtained from UPS spectra.

	E_f (eV)	E_{offset} (eV)	HOMO (eV)	ΔE (eV)	E_{ID} (eV)
ITO[1]	-4.32	-	-	-	-
p-TAPC	-4.21	0.99	-5.20	0.20	-
ML-TAPC	-4.68	0.71	-5.39	**0.01**	0.36
p-PTAA	-4.81	0.51	-5.32	0.08	-
ML-PTAA	-4.89	0.48	-5.37	**0.03**	0.57
p-PEDOT:PSS	-4.79	0.23	-5.02	0.38	-
ML-PEDOT:PSS	-5.09	0.18	-5.27	**0.13**	0.77
MAPbI$_{3-x}$Cl$_x$[1]	-4.60	0.80	-5.40	-	-

Table S2. Fitted parameters of TRPL spectra for perovskite grown on different substrates.

	A_1 (%)	τ_1 (ns)	A_2 (%)	τ_2 (ns)	τ_{ave} (ns)
ITO/Perovskite	28.8	31.4	65.0	71.5	65.0
p-TAPC/Perovskite	50.9	12.8	49.6	34.3	28.3
ML-TAPC/Perovskite	40.0	12.0	60.0	12.0	12.0

The TRPL spectra were fitted by a bi-exponential decay function,

$$I(t) = A_1 e^{-t/\tau_1} + A_2 e^{-t/\tau_2}$$

and the average PL lifetime is calculated by

$$\tau_{ave} = \frac{A_1 \tau_1^2 + A_2 \tau_2^2}{A_1 \tau_1 + A_2 \tau_2}$$

Table S3. Summary of photovoltaic parameters of devices based on the investigated HTLs.

	V_{oc} (V)	J_{sc} (mA/cm^2)	FF (%)	PCE (%)	R_s ($\Omega \cdot$cm^2)	R_{sh} (k$\Omega \cdot$cm^2)
p-TAPC	1.10	22.66	78.82	19.62	1.5	4.2
	1.10 ± 0.01	21.84 ± 0.57	77.21 ± 2.04	18.53 ± 0.65		
ML-TAPC	1.10	22.77	81.86	20.58	1.1	5.8
	1.10 ± 0.00	21.95 ± 0.46	80.43 ± 1.16	19.45 ± 0.46		
p-PTAA	1.09	22.10	78.83	19.02	1.6	4.5
	1.08 ± 0.01	21.47 ± 0.45	78.90 ± 0.87	18.34 ± 0.46		
ML-PTAA	1.09	21.83	80.30	19.16	1.2	5.3
	1.09 ± 0.01	21.56 ± 0.32	79.29 ± 0.94	18.62 ± 0.34		
p-PEDOT:PSS	1.02	21.16	77.30	16.68	2.1	3.8
	1.00 ± 0.01	20.25 ± 0.66	76.24 ± 1.92	15.38 ± 0.70		
ML-PEDOT:PSS	1.02	20.59	80.33	16.86	1.5	4.9
	1.01 ± 0.01	20.79 ± 0.47	77.39 ± 1.15	16.18 ± 0.50		

Table S4. Summary of photovoltaic parameters of champion devices with forward and reverse scan.

		V_{oc} (V)	J_{sc} (mA/cm^2)	FF (%)	PCE (%)
p-TAPC	Forward	1.10	22.66	78.82	19.62
	Reverse	1.09	22.69	73.45	18.20
ML-TAPC	Forward	1.10	22.77	81.86	20.58
	Reverse	1.10	22.68	79.65	19.89

Table S5. Hysteresis index calculated from the best devices based on p-TAPC and ML-TAPC.

		V_{oc} (V)	J at 80% of V_{oc} (mA/cm^2)	Hysteresis index
p-TAPC	Forward	1.10	21.72	0.059
	Reverse	1.09	20.51	
ML-TAPC	Forward	1.10	22.26	0.028
	Reverse	1.10	21.65	

The hysteresis index in calculated by

$$Hysteresis\ index = \frac{J_{RS}(0.8V_{oc}) - J_{FS}(0.8V_{oc})}{J_{RS}(0.8V_{oc})}$$

where J_{RS} (0.8V_{oc}) and J_{FS} (0.8V_{oc}) represent photocurrent density at 80% of V_{oc} for the reverse scan (RS) and forward scan (FS), respectively.[2]

Table S6. Photovotic parameters of devices based on PTAA with various rinsing times, measured under AM1.5G illumination (100 mW cm^{-2}).

Times	V_{oc} (V)	J_{sc} (mA/cm^2)	FF (%)	PCE (%)
0	1.09	22.10	78.83	19.02
	1.08 ± 0.01	21.47 ± 0.45	78.90 ± 0.87	18.34 ± 0.46
1	1.09	21.83	80.30	19.16
	1.09 ± 0.01	21.56 ± 0.32	79.29 ± 0.94	18.62 ± 0.34
5	1.09	21.65	80.22	18.91
	1.09 ± 0.01	21.51 ± 0.35	79.17 ± 1.78	18.56 ± 0.25

Data obtained by averaging 10 optimized devices

Reference

1. W. Kong, W. Li, C. Liu, H. Liu, J. Miao, W. Wang, S. Chen, M. Hu, D. Li, A. Amini, S. Yang, J. Wang, B. Xu, C. Cheng, *ACS Nano* **2019**, *13*, 1625.
2. H.-S. Kim, N.-G. Park, *J. Phys. Chem. Lett.* **2014**, *5*, 2927.